Synthesis, In Vivo Evaluation and PET Study of a Carbon-11-Labeled Neuronal Nitric Oxide Synthase (nNOS) Inhibitor S-Methyl-L-Thiocitrulline

Jian Zhang, Ming Xu, Carmen S. Dence, Elizabeth L.C. Sherman, Timothy J. McCarthy and Michael J. Welch

Mallinckrodt Institute of Radiology, Washington University Medical School, St. Louis, Missouri

Reports have implicated neuronal nitric oxide synthetase (nNOS) in the pathological effects of neurodegenerative diseases. S-Methyl-L-thiocitrulline (MTICU), a potent and selective nNOS inhibitor (K_i=1.2 nM), was chosen as our initial target molecule for positron emitter labeling as a potential nNOS tracer. We report the synthesis, biological evaluation and primate brain images of S-[^{11}C]methyl-L-thiocitrulline ([^{11}C]MTICU). **Methods:** The two-step synthesis of [^{11}C]MTICU consisted of the S-alkylation of α-N-Boc-L-thiocitrulline t-butyl ester with [^{11}C]MeI followed by TFA hydrolysis and HPLC purification. The final product was obtained within 50 min (yield = 9.1%–12.5%, based on [^{11}C]MeI S.A.=27–680 Ci/mmol at end of synthesis). The lipophilicity of [^{11}C]MTICU was determined by octanol/water partition coefficient (LogP). Blood stability of this tracer in vitro and in vivo was measured by HPLC analysis. Biodistribution using female Sprague-Dawley rats was performed, including examination of uptake in cerebellum and olfactory bulb (high nNOS) as well as cortex and brain stem (low nNOS). Carbon-11-MTICU was administered to a female baboon and brain images were obtained using a Siemens ECAT EXACT scanner for determination of brain regional uptake and blood-brain barrier permeability. **Results:** At 30 min postinjection, [^{11}C]MTICU remained 64% intact in vivo and 95% intact in vitro. Lipophilicity estimation gave Log p = 1.08 ± 0.08 (n = 6). The brain (0.11% ID/g)-to-blood (0.20% ID/g) ratio was 1:2 at 30 min postinjection. Uptake in the cerebellum was 20% higher than in either the cortex or the brain stem (p < 0.05). Blockage using 1 mg/kg MTICU reduced uptake in the cerebellum and the cortex by 22%, but did not affect the brain stem. PET imaging showed that [^{11}C]MTICU brain uptake, corrected for blood volume, was stable from 10 min to 1 hr at approximately 0.4% ID/organ. PET images of a baboon brain showed increased uptake in the region of the olfactory bulb compared to uniform biodistribution in the rest of the brain. **Conclusion:** The [^{11}C]MTICU is a tracer that is potentially useful in determining nNOS levels in vivo.

Key Words: nitric oxide synthtase; PET; carbon-11-MTICU

J Nucl Med 1997; 38:1273–1278

$\mathbf{N}$itric oxide (NO) is a short-lived radical that is involved in regulatory processes including vasorelaxation, neurotransmission and cytotoxicity (*1,2*). This radical is generated in biological systems from L-arginine by either constitutive (cNOS) or inducible (iNOS) nitric oxide synthase (*3,4*). The cofactor Ca^{2+}/calmodulin is required by cNOS with one subtype located predominantly in the vascular endothelium (eNOS) and another in the brain (nNOS) and peripheral nerve cells. iNOS is induced as a response to cytokines or endotoxin in various tissues and is associated with host defense mechanisms.

Our previous work (*5*) has emphasized the development of PET tracers for probing iNOS activity in vivo. Several potent and selective iNOS inhibitors, S-methyl-, S-2-fluoroethyl- and S-ethyl-isothioureas, have been labeled with ^{11}C and ^{18}F. These

labeled inhibitors have been evaluated in vitro in cell uptake assays and in vivo in a rat model. The initial results suggest that this first generation of radiolabeled inhibitors may be useful for assessing the levels of iNOS in vivo with PET. As an extended effort, the development of PET tracers for nNOS is the focus of this paper.

Overproduction of NO has been implicated in the pathological effects of neurodegenerative diseases (*6–9*). Although the mechanism of this pathology remains to be clarified, increasing evidence has suggested the involvement of nNOS. Rapid upregulation of nNOS in brain ischemic lesions (*10*) and in spinal neurons after avulsion (*11*) has been observed. Recent studies in nNOS knockout mice have indicated that highly activated nNOS contributes to CNS tissue damage in cerebral ischemia, whereas eNOS may protect brain tissue by increasing ischemic regional blood flow (*12*). Selective inhibition of nNOS for the treatment of neurodegenerative diseases is suggested.

The development of positron-emitting radionuclide-labeled nNOS tracers holds the potential of providing a molecular probe for noninvasively detecting nNOS activity in normal or diseased states. This will aid in elucidating the role of nNOS in the brain as well as evaluating the effects of novel pharmaceuticals on the enzymatic systems in vivo.

Several nNOS selective inhibitors (Fig. 1) have been reported (*1,13,14*). S-Methyl-L-thiocitrulline (MTICU) is the most potent and selective nNOS inhibitor (K_i = 1.2 nM) among them (*15,16*). S-Methyl-L-thiocitrulline showed a 40-fold selectivity for nNOS compared to eNOS and 11-fold selectivity compared to iNOS in enzyme assays. It exhibited a 17-fold selectivity for nNOS compared to eNOS in tissue assays. MTICU has also been reported recently to reduce the size of infarction in a focal cerebral ischemia rat model (*16*). In addition, MTICU has been shown to be a competitive inhibitor of nNOS; it inhibits the enzyme by occupying the enzyme's active site. Therefore, MTICU was chosen as our initial target nNOS inhibitor for labeling with a positron emitter. We report here the synthesis, biological evaluation and primate brain images of the ^{11}C-labeled nNOS inhibitor S-methyl-L-thiocitrulline.

MATERIALS AND METHODS

Unless otherwise stated all chemicals were obtained from Aldrich Chemical Co. (Milwaukee, WI). N^{α}-tert-Butoxycarbonyl-L-thiocitrulline tert-butyl ester and S-methyl-L-thiocitrulline (MTICU) were prepared according to literature methods (*17,18*). HPLC for the radiochemical experiments was performed on a Spectra-Physics 8700 chromatograph (San Jose, CA) equipped with a Whatman Partisil 10 SCX HPLC column (Fairfield, NJ), a Waters UV detector (Lambda-Max Model 480, Milford, MA, operating at 242 nm), a well scintillation NaI(Tl) scintillation detector with associated electronics, and a fraction collector. The HPLC conditions used in this work were the following: Condition
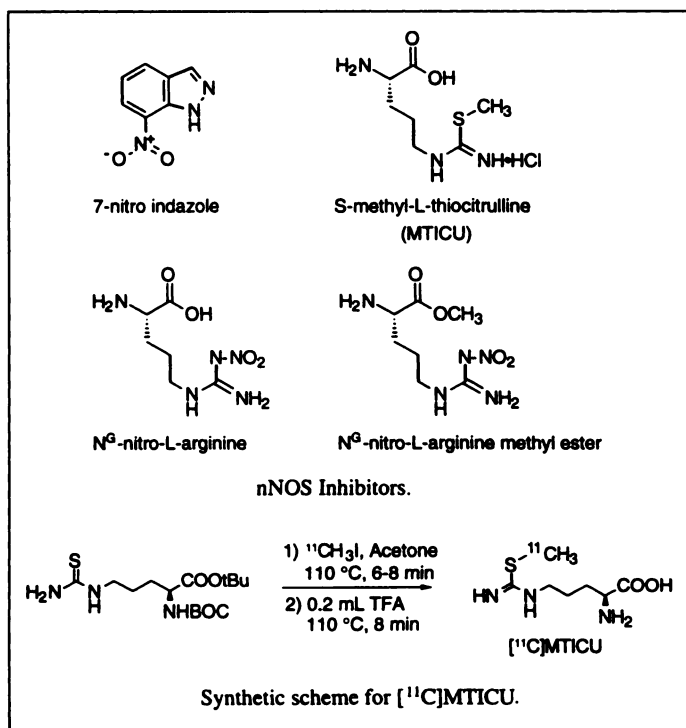
FIGURE 1. (A) nNOS inhibitors. (B) Synthetic scheme for [^{11}C]MTICU.

A for purification and stability studies of the radiolabeled product, a semipreparative column (0.9 × 50 cm, Mag 9) eluted isocratically with solvent of 5.0% ethanol in 0.10 N saline at a flow rate of 5 ml/min; and Condition B for the determination of radiochemical purity and specific activity of the radiolabeled product, an analytical column (0.46 × 25 cm) eluted isocratically with 5% acetonitrile in 0.05 N saline at a flow rate of 2 ml/min. For serum stability studies and biodistribution studies, radioactivity was determined on an automatic well scintillation gamma counter (Gamma 8000, Beckman, Irvine, CA).

Two imaging studies were performed with a Siemens/CTI (Knoxville, TN) ECAT EXACT47 scanner in the two-dimensional mode. This scanner acquires 47 simultaneous slices at a section interval of approximately 3.4 mm over an axial extent of 16.2 cm. This tomograph has an intrinsic resolution 6.2 mm (FWHM) in the axial direction. Reconstructed inplane transaxial resolution is approximately 11 mm (FWHM).

Preparation of Carbon-11-MTICU

Carbon-11-MTICU was synthesized as shown in Figure 1B. (19). The synthetic precursor, [^{11}C]methyl iodide, was prepared from either a previously reported remote gantry system (20) or from a PETtrace MeI microlab (General Electric, PET Systems AB, Uppsala, Sweden) (21). The [^{11}C]methyl iodide prepared by remote gantry system was synthesized by the reaction of [^{11}C]methanol with HI, in which [^{11}C]methanol was produced from reduction of [^{11}C]CO$_2$ with LiAlH$_4$ in THF. The PETtracer MeI microlab from General Electric generates [^{11}C]methyl iodide from the reaction of [^{11}C]methane with iodine, in which [^{11}C]methane was obtained from the catalytic hydrogenation of [^{11}C]CO$_2$ with H$_2$ (gas). In both cases, the [^{11}C]methyl iodide formed was passed by a drying tube filled with KOH pellets and P$_2$O$_5$ powder, and trapped at 0°C in a 2-ml conical vial containing 1 ml acetone. The collected [^{11}C]methyl iodide was transferred to a 2-ml Reactivial® (Wheaton, Millville, NJ) with 2 mg of N$^\alpha$-tert-butoxycarbonyl-L-thiocitrulline tert-butyl ester prepared according to Feldman's procedure (17). The mixture was refluxed at 110°C for 6–8 min. After the solvent was evaporated under nitrogen, the reaction

mixture was further hydrolized in 200 μl TFA at 110°C for 8 min. The residue was dissolved in 2 ml HPLC solvent and purified by HPLC Condition A. The desired product [^{11}C]MTICU, retention time 13.2 min, was collected for further study. Thiocitrulline eluted just after the solvent front. The total synthesis and purification was achieved within 50 min from the [^{11}C]methyl iodide delivery, and radiochemical yield ranged from 9.1%–12.5% (based on [^{11}C]CH$_3$ I) at end of synthesis. The radiochemical purity of [^{11}C]MTICU was determined by analytical SCX HPLC Condition B to be greater than 99%. Specific activity (SA) was determined by comparison of UV absorbance with that of known standards to be 27–680 Ci/mmol at end of synthesis, with the higher values obtained by using [^{11}C]methyl iodide produced on the PETtrace system. The identity of the tracer was confirmed by the co-elution of [^{11}C]MTICU with nonradioactive standard on the analytical HPLC system.

Determination of the Partition Coefficient (Log P)

The partition coefficient for [^{11}C]MTICU was measured as follows. A 20-μCi sample of radiolabeled compound (volume less than 50 μl) in 5% EtOH/0.10 N saline was added to a premixed suspension of 1 ml octanol in 1 ml water. The resulting solution was mixed for 30–45 sec and centrifuged for 5 min at 2000 rpm. An 800 μl aliquot of the octanol layer was removed and extracted with 800 μl water. The solution was mixed and centrifuged as before. A 500 μl aliquot of the octanol layer was removed and extracted with 500 μl of water. The radioactivity of each layer of the back extraction was measured. Each octanol and water layer was weighed. The partition coefficient was calculated as the ratio of CPM/g of octanol to CPM/g of water per extraction. Experiments were conducted in quadruplicate. The average log P value of the two back extractions for the four trials is reported.

In Vitro and In Vivo Stability Study

In vivo and in vitro stability studies for [^{11}C]MTICU were performed. In the in vivo experiments, the radiotracer (2 mCi/rat, S.A.= 50 Ci/mmol) was injected into the tail vein of the anesthetized mature female Sprague-Dawley rats (150–200 g). Blood samples were obtained by cardiac puncture at various time points postinjection and centrifuged for 2 min at 14,000 rpm. The plasma was separated from the red blood cell pellet and analyzed by HPLC with the semiprep SCX column. HPLC fractions were collected and activity was counted. Radioactivity balance was determined by comparing injected activity with total activity eluted from the column. The in vitro studies were performed by adding the radiotracer (dissolved in 0.3 ml 0.1 N NaCl) to 3 ml fresh rat blood. The mixture was incubated at 37°C and 100-μl aliquot samples were withdrawn at specific time points for analysis as described above.

Biodistribution Studies

Biodistribution studies were performed in mature female Sprague-Dawley rats (150–200 g). Radiolabeled tracer, [^{11}C]MTICU in saline solution, was administered to the rats under methoxyflurane anesthesia by tail vein injection. The injected radioactive dose was approximately 50 μCi/rat with specific activity of 73 Ci/mmol. The animals were allowed free access to water and food. At specific time points post-tracer administration, the rats were reanesthetized and killed by decapitation. The organs and tissues of interest were removed and weighed. The radioactivity levels in the sampled organs/tissues were determined. The percent injected dose per gram of tissue (%ID/g) was calculated by comparison to a weighed and counted standard solution.

Rat Brain Biodistribution Studies

Both a control and a blocking group of mature female Sprague-Dawley rats (n = 4) were used in the experiments. Carbon-11-

MTICU (30 μCi/rat, SA = 37 Ci/mmol) was administered to the rats under Metafane® anesthesia by tail vein injection for the control group. For the blocking group, an additional 1 mg/kg MTICU was coinjected with the tracer as a blocking agent. The biodistribution of [^{11}C]MTICU in both groups were determined as described above.

PET Imaging

A mature female baboon (17.1 kg, 12 yr old) was used in the PET study. The baboon was anesthetized (15–20 mg/kg ketamine; xylazine 0.25 mg/kg; 0.2 mg atropine sulfate) before the study began. Anesthetization was maintained by further administration of ketamine (10 mg/kg) as necessary. A 20-gauge plastic catheter was inserted into a femoral artery to permit arterial blood sampling. The animal was placed supine in a U-shaped acrylic holder and was given a continuous intravenous saline drip (400–500 ml total). The head of the baboon was fixed in place by a head brace. The head was positioned with the aid of a vertical line projected from a laser permanently fixed on the wall. The line coincided with the center of the lowest PET slice when the scanning table was completely advanced into the scanner.

Attenuation characteristics of the head were determined before each study by obtaining a transmission scan using a ^{68}Ge/^{68}Ga rotating rod source. Regional cerebral blood volume (rCBV) was measured in a 5-min PET scan after the inhalation of [^{15}O]carbon monoxide. Regional cerebral blood flow (rCBF) was measured using a 40-sec scan after the intravenous injection of 20–30 mCi of [^{15}O]water. Sequential PET scans commenced with the intravenous injection (in a vein of the foreleg) of [^{11}C]MTICU (6.8 mCi, SA = 140 Ci/mmol; 10.25 mCi, SA = 680 Ci/mmol) and continued for 1 hr (acquisition frames: 12 × 10 sec; 12 × 30 sec; 10 × 60 sec; 10 × 240 sec) for the two separate PET studies. Arterial blood samples (0.5 ml) were collected every 10 sec for the first 2 min and then with decreasing frequency to every 2–10 min during the remainder of the study. Blood samples were weighed and radioactivity levels determined. The percent injected dose per gram of blood (%ID/g) was calculated by comparison to a counted standard solution.

RESULTS

Radiochemical Synthesis

The synthesis of [^{11}C]MTICU was accomplished in two steps from the synthetic precursor α-N-Boc-L-thiocitrulline t-butyl ester by thioalkylation with [^{11}C]MeI followed by TFA hydrolysis (Fig. 1B). The final product was obtained within 50 min with good radiochemical purity and yield (yield = 9.1%–12.5% at end of synthesis). The specific activity of [^{11}C]MTICU was dependent on the [^{11}C]MeI source; it was in the range of 27–143 Ci/mmol and 343–680 Ci/mmol (at end of synthesis) when using [^{11}C]MeI prepared from a remote gantry system and PETtrace MeI microlab, respectively. Final product yield was affected by the incorporation of [^{11}C]MeI. Incorporation of [^{11}C]MeI was improved by increasing the reaction temperature to 110°C and extending the reaction time to 6–8 min. From our observation, the higher the [^{11}C]MeI specific activity, the longer the incorporation time is required. This is possibly due to a greater fraction of activity being in the head space above the reaction mixture at the higher specific activity. Removal of solvent after the S-alkylation followed by TFA hydrolysis gave the final product within 8 min and in greater than 90% yield for the second step.

Partition Coefficients (Log P)

The average log P value of the two back extractions for the four trials was 1.09 ± 0.08. Neutral compounds with this lipophilicity (22) have very high blood-brain barrier extraction,
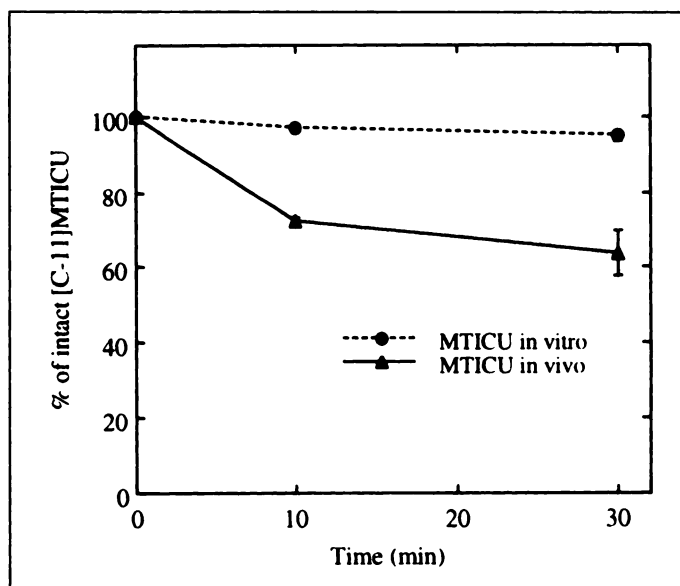

FIGURE 2. Percent unmetabolized [^{11}C]MTICU remaining in the rat serum in vivo and in vitro versus time. Data are average of two experiments; results are expressed as mean ± sd; n = 2.

however, maximum extraction of a series of acids was observed at log P ∼ 2.72. (23) Citrulline itself has been found to have very low brain uptake. (24)

Stability Study

To determine the biological half-lives of [^{11}C]MTICU in vivo and in vitro, plasma samples were taken after the tracer administration and were analyzed using SCX HPLC, at times from 5–30 min, the amount of activity extracted into the plasma was constant (74% ± 3%). Carbon-11-MTICU remained 72% intact in vivo and 97% intact in vitro at 10 min; after 30 min, [^{11}C]MTICU was 64% intact in vivo and 95% intact in vitro. Only two peaks were observed by HPLC, [^{11}C]MTICU and a peak at the origin. Attempts were made to investigate this product, it was not volatile and studies using size exclusion membranes showed that < 10% was protein bound. All the radioactivity was accounted for. Detailed stability versus time curves for [^{11}C]MTICU are shown in Figure 2.

Biodistribution Studies

In vivo biodistribution results of no-carrier-added [^{11}C]MTICU in mature female Sprague-Dawley rats are presented in Table 1. The [^{11}C]MTICU demonstrated some brain penetration. It showed slow clearance in brain, muscle and liver. Rapid clearance of this tracer was seen in the blood, lung, heart and

TABLE 1
Biodistribution of Carbon-11-MTICU in the Mature Female Sprague-Dawley Rat*

Organ/Tissue	%ID/g ± s.d. (n = 4)		
	5 min	15 min	30 min
Blood	0.87 ± 0.11	0.43 ± 0.04	0.20 ± 0.01
Lung	0.82 ± 0.08	0.51 ± 0.03	0.29 ± 0.02
Liver	0.93 ± 0.07	0.68 ± 0.14	0.69 ± 0.02
Kidney	2.74 ± 0.15	1.92 ± 0.18	1.19 ± 0.09
Muscle	0.32 ± 0.01	0.35 ± 0.01	0.26 ± 0.01
Heart	0.65 ± 0.03	0.39 ± 0.02	0.24 ± 0.01
Brain	0.16 ± 0.02	0.13 ± 0.01	0.11 ± 0.01
Ab aorta	0.86 ± 0.04	0.49 ± 0.07	0.25 ± 0.01

*Each rat was administered 50 μCi of [^{11}C]MTICU (S.A. = 73 Ci/mmol).

kidney. The brain-to-blood ratio reached 1:2 at 30 min post-injection.

Rat Brain Biodistribution Studies

Four brain regions, cerebellum, olfactory bulb, cortex and brainstem, were examined for [^{11}C]MTICU uptake at 30 min postinjection (Table 2). Higher uptake was observed in the cerebellum and olfactory bulb compared to that in the cortex and brain stem. Uptake in the cerebellum was significantly higher (p < 0.01) than that of the cortex and brain stem. In the blocking experiment, the cerebellum- and cortex-uptake levels decreased by 20%, but the activity remained constant in the brainstem. Brain samples (30 min post-injection) were extracted with HPLC solvent B. A total of 58% ± 2% of the activity was extracted and HPLC analysis showed 74% of this activity to be [^{11}C]MTICU.

PET Imaging

To assess the brain uptake and brain regional distribution of [^{11}C]MTICU, we performed two experiments to examine the tracer uptake in the intact brain of a normal primate using PET. Both PET studies exhibited very similar results, therefore the images and data from only one experiment are shown here. Figure 3 shows reconstructed transaxial images of baboon brain. Higher activity was observed in surrounding tissues than in the brain. The total brain uptake of [^{11}C]MTICU was constant from 10 min to 1 hr, remaining at approximately 0.4% ID/brain, corrected for blood volume (Fig. 4). Although uniform biodistribution of [^{11}C]MTICU was observed in the gray and white matter of the brain, higher activity was detected in the region of the olfactory bulb (Figs. 5 and 6). This was done by visual inspection of images in transaxial, sagittal and coronal directions and comparison with the known anatomy of the baboon brain. Activity accumulation was noticed in the thyroid, and was about twice the activity in the blood or the olfactory bulb (Fig. 7). Time-activity curves for the tracer, measured by sampling the arterial blood, indicated that [^{11}C]MTICU cleared from the blood rapidly. Only 5% of injected activity remained in whole blood at 1 hr postinjection (Fig. 8).

TABLE 2
Uptake of Carbon-11-MTICU in Brain Regions of the Mature Female Sprague-Dawley Rat at 30 min*

Organ/Tissue	%ID/g ± s.d. (n = 3)	
	Control	Blocking (1 mg/kg)
Blood	0.22 ± 0.03	0.24 ± 0.02
Muscle	0.28 ± 0.01	0.30 ± 0.02
Cerebellum	0.13 ± 0.00†	0.10 ± 0.01‡
Olfactory bulb	0.15 ± 0.04	0.10 ± 0.01
Cortex	0.10 ± 0.01	0.08 ± 0.01‡
Brain stem	0.10 ± 0.01	0.10 ± 0.01

*Each rat was administered 30 μCi of [^{11}C]MTICU (S.A. = 37 Ci/mmol).
†Uptake in cerebellum is significantly higher (p < 0.01) than that of the cortex and brain stem.
‡Compared to the control, uptake was reduced in the cerebellum (p < 0.004) and cortex (p < 0.04) with administration of 1 mg/kg MTICU.

DISCUSSION

In the rat and primate brain, nNOS activities and protein levels are high in the cerebellum and olfactory bulb region, and low in the cortex and brain stem (25). Evaluation of radiotracer uptake in the high as well as low nNOS regions gives an indication of its relative target to non target localization. In vitro autoradiographic studies using N^G-nitro-L-[2,3,4,5-^{3}H]arginine, a tritiated nNOS selective inhibitor, have shown its specific binding to nNOS in olfactory bulb and cerebellum (26,27).

In our biodistribution studies, [^{11}C]MTICU showed that uptake in the cerebellum was approximately 20% higher (p < 0.01) than in the cortex and brain stem. The olfactory bulb had the highest uptake; however, due to large errors in the absolute value, the value was not statistically different from the uptake of the cortex, brain stem or cerebellum. The stability of MTICU was evaluated in vitro and in vivo in the blood and brain. The compound was very stable in vitro and up to 30 min postinjection. The majority of activity in the blood and brain was authentic [^{11}C]MTICU. A similar stability trend has been observed for the nonselective NOS inhibitor [^{11}C]-S-methyl isothiourea (5), this compound is structurally similar to MTICU
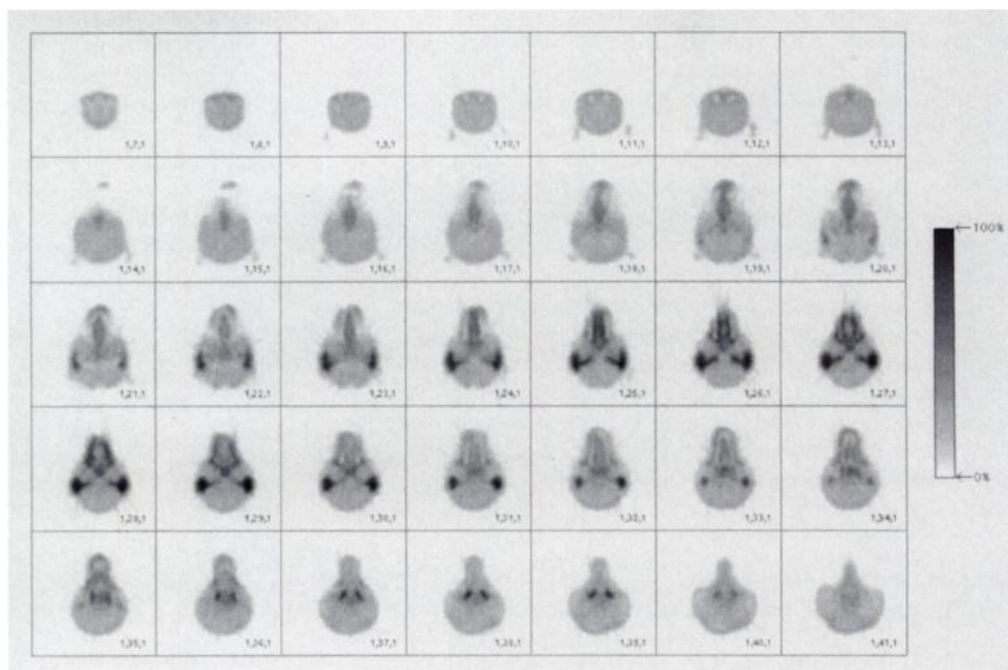

FIGURE 3. PET-reconstructed transaxial images of a baboon brain after administration of 6.8 mCi [^{11}C]MTICU (SA = 140 Ci/mmol). The images are taken from 5 to 10 min.
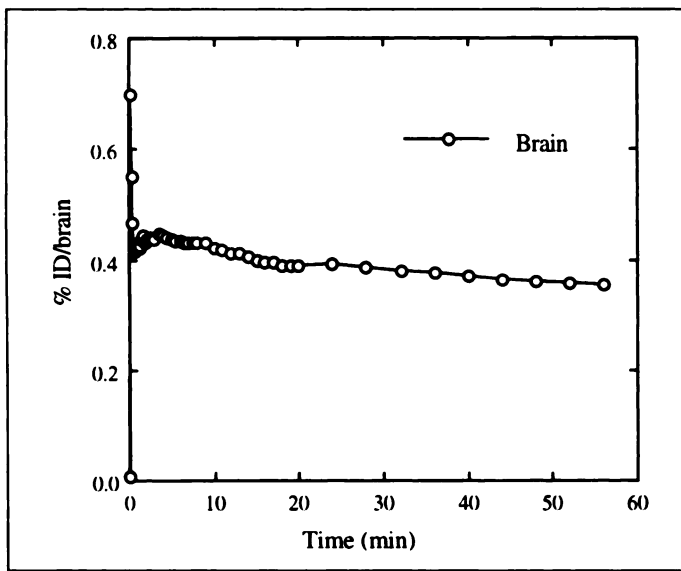
FIGURE 4. Percent injected dose of [¹¹C]MTICU in the brain. Decay-corrected time-activity curve generated from sequential PET images of the brain.

FIGURE 6. Comparision of [¹¹C]MTICU uptake (%ID/ml x 10⁻³) in olfactory bulb, cerebellum, white matter and gray matter of a baboon brain. Decay-corrected time-activity curve generated from sequential PET images of the brain.

and this also appears to be stable in vivo over the time period of studies using ¹¹C. When 1 mg/kg MTICU was coadministered in the rat model in the blocking experiment, cerebellum- and cortex-uptake levels decreased by 20%, but the activity remained constant in the brain stem. Blocking removed the significant difference in uptake in the cerebellum compared to the cortex and brain stem.

Since only limited [¹¹C]MTICU uptake was observed in the rat brain, it was not known whether this activity was associated with the brain or with the vascular wall. This can be determined by comparing PET images of [¹¹C]MTICU to that of [¹⁵O]CO in a primate brain. Since [¹⁵O]CO is a blood volume tracer, [¹¹C]MTICU should have similar brain imaging patterns if [¹¹C]MTICU were stuck to the vascular wall. In addition, PET imaging provides a means to assess brain regional distribution (28–30) of [¹¹C]MTICU.

Different brain images of [¹¹C]MTICU from [¹⁵O]CO were

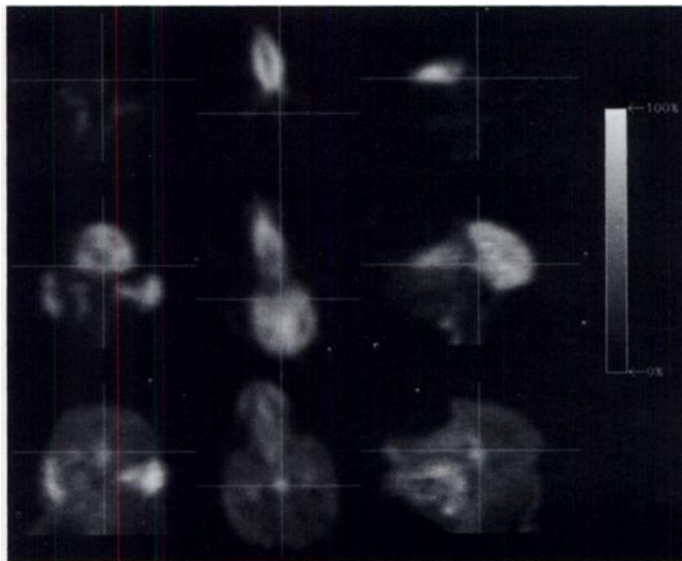observed, which suggests that [¹¹C]MTICU, instead of being associated with the brain vascular wall, did penetrate the blood-brain barrier. After correcting for blood volume, total activity in the brain was calculated to be approximately 0.4% of injected dose. Higher uptake (>50% higher) was observed only in the olfactory bulb, known to contain nNOS (25), compared to the rest of the brain in which uniform distribution was observed. In addition, [¹¹C]MTICU showed similar rapid blood clearance patterns in both rats and the baboon. In rats, the activity cleared the blood within 30 min to 2% of the injected dose, while the activity remained at 5% injected dose in the baboon blood up to 1 hr.

Significant differences in nNOS enzymatic activity as well as in nNOS protein levels have been reported for the various brain regions; however, [¹¹C]MTICU uptake only displayed moderate uptake differences in these regions. This may be attributed to several factors. First, L-arginine has been reported in blood

FIGURE 5. PET images of a baboon brain after administration of [¹⁵O]CO (top row), [¹⁵O]H₂O (middle row) and [¹¹C]MTICU (bottom row, images of 40–60 min). Coronal (left), transaxial (middle) and sagittal (right) PET images of three tracers on the same slice are displayed. The position of the olfactory bulb is indicated by the point of intersection of the lines.
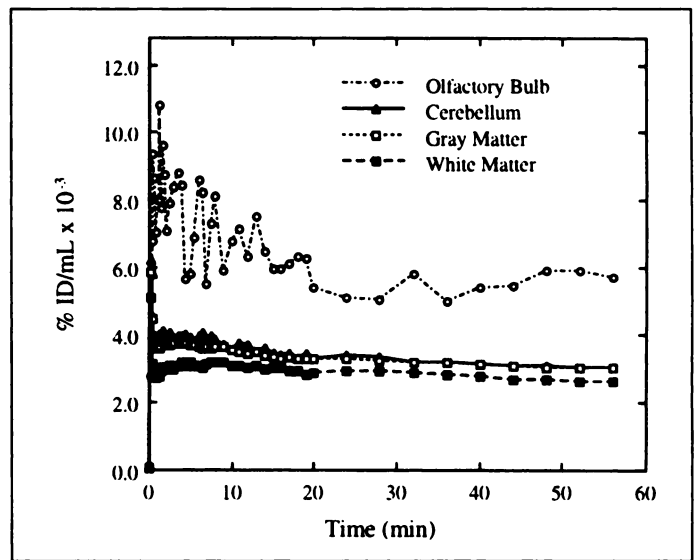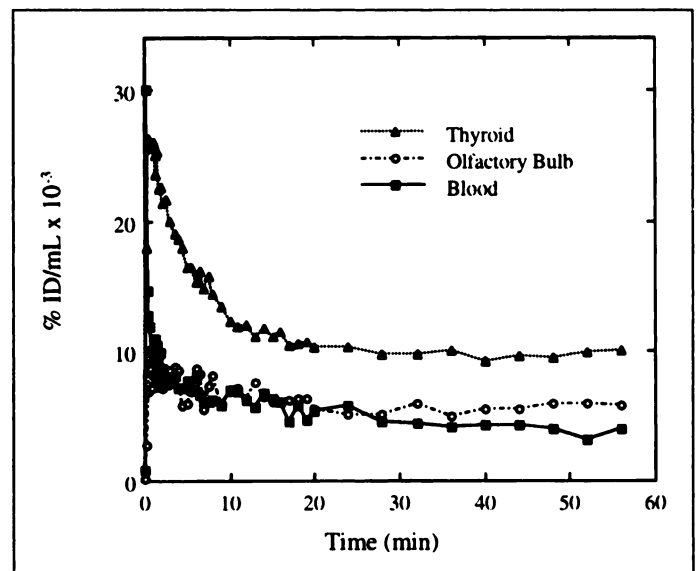

FIGURE 7. Comparision of [¹¹C]MTICU activity (% ID/ml x 10⁻³) in the thyroid, olfactory bulb and blood. Decay-corrected time-activity curve generated from sequential PET images.
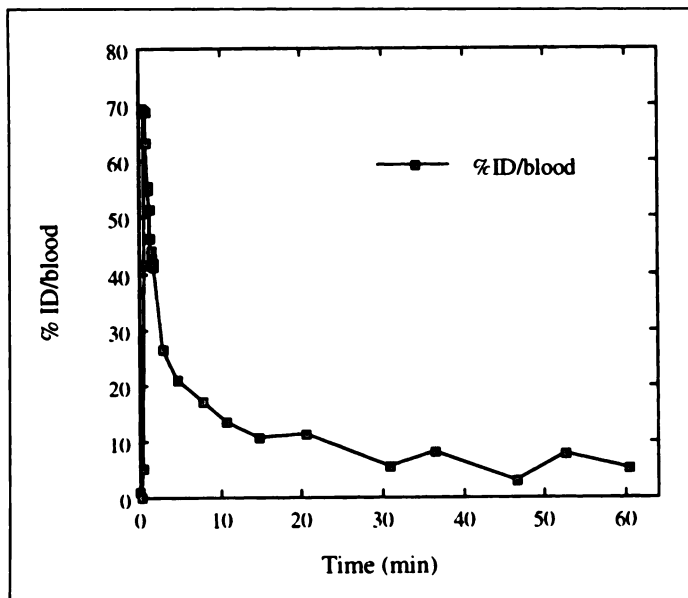
FIGURE 8. Time-blood activity curve of [^{11}C]MTICU plotted as the percent injected dose in the whole-blood volume (% ID/blood). Data were generated from arterial blood sampling. Total blood volume calculated to be approximately 1200 ml based on blood weight of about 7% body weight (7% × 17.1 kg = 1.2 kg, assuming blood density = 1 g/ml).

plasma of adult humans in the range of 40–120 mM (*31*), with similar levels reported in the brain (*32*). MTICU has an affinity (K_i) for nNOS at least 1000 times higher than the K_m of arginine (2 μM). At these physiological arginine concentrations, competition may occur and reduce the contrast. In addition, low blood-brain barrier permeability of [^{11}C]MTICU (0.4% injected dose/brain) may hamper its accessibility to the target.

However, this low permeability may not prove to be a great impedence, as [^{18}F]spiperone, the dopamine radiotracer previously developed in our lab, has shown similar uptake in the rat brain (*33*). [^{18}F]Spiperone has been shown to be an effective tracer for study of dopaminergic receptor binding in vivo in humans despite its relatively low permeability (*34*). Finally, nNOS activity is controlled by a cofactor, calcium/camodulin, and is only intermittently activated by transient elevations in intracellular calcium levels. Under normal physiological conditions, nNOS is not highly activated, therefore, [^{11}C]MTICU may not be able to distinguish normal levels of brain nNOS. Consequently, the fate of [^{11}C]MTICU as an nNOS tracer will depend on its further evaluation in the diseased state in which nNOS is upregulated and highly activated.

We have achieved the synthesis of the first neuronal NOS inhibitor [^{11}C]MTICU by thioalkylation of α-N-Boc-L-thiocitrulline t-butyl ester with [^{11}C]MeI followed by TFA hydrolysis. Tissue distribution studies in rats have shown higher uptake in the brain regions where nNOS is found in highest concentrations. PET images of a baboon brain showed increased uptake in the olfactory bulb compared to uniform biodistribution in the rest of brain. Further evaluation of [^{11}C]MTICU in an animal model in which nNOS is highly activated is indicated.

ACKNOWLEDGMENTS

REFERENCES

1. Moncada S, Palmer RMJ, Higgs EA. Nitric oxide: physiology, pathophysiology and pharmacology. *Pharmacol Rev* 1991;43:109–142.
2. Nathan CF. Nitric oxide as a secretory product of mammalian cells. *FASEB* 1992;6:3051–3064.
3. Stuehr DJ, Griffith OW. Mammalian nitric oxide synthases. *Adv Enzymol Relat Mol Biol* 1992;65:287–346.
4. Marletta MA. Nitric Oxide Synthase structure and mechanism. *J Biol Chem* 1993;268:12231–12234.
5. Zhang J, McCarthy TJ, Moore WM, Currie MG, Welch MJ. Synthesis and evaluation of two position-labeled nitric oxide synthase inhibitors, S-[^{11}C]methylisothiourea and S-(2-[^{18}F]fluoroethyl)isothiourea, as potential position emission tomography tracers. *J Med Chem* 1996;39:5110–5118.
6. Dawson VL, Dawson TM, London ED, Bredt DS, Snyder SH. Nitric oxide mediates glutamate neurotoxicity in primary cortical cultures. *Proc Natl Acad Sci USA* 1991;88:6368–6371.
7. Nowicki JP, Duval D, Poignet H, Scatton B. Nitric oxide mediates neuronal death after focal cerebral ischemia in the mouse. *Eur J Pharmacol* 1991;204:339–340.
8. Choi DW. Nitric oxide: foe or friend to the injured brain? *Proc Natl Acad Sci USA* 1993;90:9741–9743.
9. Dawson DA. Nitric oxide and focal cerebral ischemia: multiplicity of actions and diverse outcome. *Cerebrovasc Brain Metab Rev* 1994;6:299–324.
10. Zhang ZG, Chopp M, Gautam S, et al. Upregulation of neuronal nitric oxide synthase and mRNA, and selective sparing of nitric oxide synthase-containing neurons after focal cerebral ischemia in rat. *Brain Res* 1994;654:85–95.
11. Wu W, Liuzzi FJ, Schinco FP, et al. Neuronal nitric oxide synthase is induced in spinal neurons by traumatic injury. *Neuroscience* 1994;61:719–726.
12. Huang Z, Huang PL, Panahian N, Dalkara T, Fishman MC, Moskowitz MA. Effects of cerebral ischemia in mice deficient in neuronal nitric oxide synthase. *Science* 1994;265:1883–1885.
13. Marletta MA. Approaches toward selective inhibition of nitric oxide synthase. *J Med Chem* 1994;37:1899–1907.
14. Kerwin JF, Lancaster JR, Feldman PL. Nitric oxide: a new paradigm for second messengers. *J Med Chem* 1995;38:4343–4362.
15. Furfine ES, Harmon MF, Paith JE, et al. Potent and selective inhibition of human nitric oxide synthases. Selective inhibition of neuronal nitric oxide synthase by S-methyl-L-thiocitrulline and. S-ethyl-L-thiocitrulline *J Biol Chem* 1994;269:26677–26683.
16. Nagafuji T, Sugiyama M, Muto A, Makino T, Miyauchi T, Nabata H. The neuroprotective effect of a potent and selective inhibitor of Type I NOS (L-MIN) in a rat model of focal cerebral ischaemia. *NeuroReport* 1995;6:1541–1545.
17. Feldman PL. Synthesis of the putative L-arginine metabolite N^G-hydroxyarginine. *Tetrahedron Letts* 1991;32:875–878.
18. Narayanan K, Griffith OW. Synthesis of L-thiocitrulline, L-homothiocitrulline, and S-methyl-L-thiocitrulline: a new class of potent nitric oxide synthase inhibitors. *J Med Chem* 1994;37:885–887.
19. Zhang J, Dence CS, McCarthy TJ, Welch MJ. Synthesis of carbon-11-labeled nitric oxide synthase (NOS) as potential NOS tracers for PET. *J Label Compound Radiopharm* 1995;37:240–242.
20. Buckman BO, VanBrocklin HF, Dence CS, Bergman SR, Welch MJ, Katzenellenbogen JA. Synthesis and tissue biodistribution of [w-^{11}C]palmitic acid. A novel PET imaging agent for cardiac fatty acid metabolism. *J Med Chem* 1994;37:2481–2485.
21. Larson P, Ulin J, Dahlström K. A new method for production of ^{11}C-labeled methyl iodide from. ^{11}C-methane. *J Label Compound Radiopharm* 1995;37:73–75.
22. Dischino DD, Welch MJ, Kilbourn MR, Raichle ME. Relationship between lipophilicity and brain extraction of C-11-labeled radiopharmaceuticals. *J Nucl Med* 1983;24:1030–1038.
23. Hansch C, Clayton JM. Lipophilic character and biological activity of drugs II: the parabolic case. *J Pharm Sci* 1973;62:1–21.
24. Oldendorf WH. Brain uptake of radiolabeled amino acids, amines and hexoses after arterial injection. *Am J Physiol* 1971a;221:1629–1639.
25. Bredt DS, Glatt CE, Hwang PM, Fotuhi M, Dawson TM, Snyder SH. Nitric oxide synthase protein and mRNA are discretely localized in neuronal populations of the mammalian CNS together with NADPH diaphorase. *Neuron* 1991;7:615–624.
26. Kidd EJ, Michel AD, Humphrey PPA. Autoradiographic distribution of [^{3}H]L-N^G-nitro-arginine binding in the rat brain. *Neuropharmacology* 1995;34:63–73.
27. Raghavendra Rao VL, Butterworth RF. Kinetics, pharmacology, and autoradiographic distribution of L-[^{3}H]nitroarginine binding sites in rat cerebellum. *J Neurochem* 1996;66:701–709.
28. Ter-Pogossian MM, Raichle ME, Sobel BE. Positron-emission tomography. *Scientific American* 1980;243:170–181.
29. Phelps ME, Mazziotta JC, Schelbert HR, eds. *Positron emission tomography and autoradiography: principles and applications for the brain and heart.* New York, NY: Raven Press; 1986.
30. McCarthy TJ, Schwarz SW, Welch MJ. Nuclear medicine and positron emission tomography: an overview. *J Chem Educ* 1994;71:830–836.
31. Sober HA, ed. *Handbook of biochemistry: selected data for molecular biology,* 2nd ed. Cleveland, OH: CRC Press Inc.; 1970:B-100.
32. Rapoport SI. *Blood-brain barrier in physiology and medicine.* New York, NY: Raven Press; 1976:191.
33. Welch MJ, Kilbourn MR, Mathias CJ, Mintun MA, Raichle ME. Comparison in animal models of ^{18}F-spiroperidol and ^{18}F-haloperidol: potential agents for imaging the dopamine receptor. *Life Sci* 1983;33:1687–1693.
34. Perlmutter JS, Kilbourn MR, Raichle ME, Welch MJ. MPTP-induced up-regulation of in vivo dopaminergic radioligand-receptor binding in humans. *Neurology* 1987;37:1575–1579.